Full Range Swept-Source Optical Coherence Tomography Using 3x3 Mach-Zehnder Interferometer with Unbalanced Differential Detection

Youxin Mao, Costel Flueraru, Sherif Sherif, and Shoude Chang*

Institute for Microstructural Sciences, National Research Council Canada,
1200 Montreal Rd, Ottawa K1A 0R6 ON, Canada
*Corresponding author: Linda.Mao@nrc-cnrc.gc.ca

ABSTRACT

We present a full range swept-source optical coherent tomography with a 3x3 Mach-Zehnder interferometer using a new unbalanced differential optical detection method. The new interferometer provides simultaneous access to complementary phase components of the complex interferometric signal. No calculations by trigonometric relationships are needed. We demonstrate a complex conjugate artifact suppression of 27 dB obtained in a swept-source optical coherence tomography using our unbalanced differential detection. We show that our unbalanced differential detection has increased the signal-to-noise ratio by 7 dB compared to the commonly used balanced detection technique. The suppression of the complex conjugate artifact in our unbalanced detection configurations were 3 dB more than in the commonly used balanced detection method. This is due to better utilization of optical power.

Index Terms— optical coherence tomography, wavelength swept-source, biomedical imaging

1. INTRODUCTION

Optical coherence tomography (OCT)[1] is becoming an increasingly important imaging tool for many applications in biology and medicine, such as diagnosis and guided surgery. In the earlier stages of the OCT imaging, axial (depth) ranging is provided by low-coherence interferometry, where the optical path length difference between the interferometer sample and reference arms are scanned linearly in time[2,3]. This method of OCT, referred to as time-domain OCT (TD-OCT) has a relatively slow imaging speed although it has demonstrated promising results for early detection of disease[4]. Fourier domain techniques in OCT have received much attention in recent years due to its significant sensitivity and high speed advantages over TD-OCT[5-7]. Fourier domain methods include spectral-domain OCT (SD-OCT) and Swept-source OCT (SS-OCT). SS-OCT is particularly important for imaging in the 1300 nm wavelength range and it also makes possible for differential detection. In SS-OCT, the location of a scatterer within tissue is obtained by a Fourier transformation of the optical measurement. When the real component of the interferometric signal is the only detected part, a complex conjugate artifact is introduced after the Fourier transformation. This artifact prevents the distinction between positive and negative object depths thereby reducing the effective imaging range by half. As imaging range is important in biomedical imaging, methods for removing this complex conjugate artifact to achieve full range in SS-OCT are of significant interest. Different full-range SS-OCT imaging methods which measure the complex component of the interferometric signal by shifting the phase of the reference and/or sample reflections have been reported. This phase shift has been implemented by a high-speed electronic-optical phase modulator[8], two high-speed acoustic-optical frequency shifters[9], and a pair of linearly polarized beams[10]. All of these methods suffered from significant image corruption resulting from any small variations in the phase shift or birefringence of used materials. Recently, acquisition of both real and imaginary interferometric components was demonstrated using Michelson quadrature interferometers using 3x3 fused fiber couplers and non-differential optical detection[11,12]. In reference [13], a 3x3 Michelson quadrature interferometer with balanced differential detection was used for acquiring the complex interferometric signal. Signal attenuation was used to achieve such balanced differential detection which resulted in loss of signal power. In their system, there was a non-complementary phase shift of 60^{o} between the two output interferometric signals that needed to be converted to quadrature components by a trigonometric manipulation. In addition, due to the nature of the Michelson interferometer, the optical output power at one of the ports of the 3x3 coupler (1/3 of the source power) was not utilized in references 11-13.

In this presentation, we present experimental results for a 3x3 Mach-Zehnder quadrature interferometer to acquire a complex interferometric signal for SS-OCT[14]. We introduce a novel unbalanced differential detection method to improve the overall utilization of optical power and provide

978-1-4244-2003-2/08/$25.00

simultaneous access to the complementary phase components of the complex interferometric signal. No calculations by trigonometric relationships are needed. We compare the performance for our setup to that of a similar interferometer with a commonly used balanced detection technique. We demonstrate complex conjugate artifact suppression of 27 dB obtained in a swept-source optical coherence tomography using our unbalanced differential detection. We show that our unbalanced differential detection has increased signal-to-noise ratio by 7 dB comparing to a commonly used balanced detection technique. The suppression of the complex conjugate artifact in our unbalanced detection configurations were 3 dB more than in the commonly used balanced detection method. This is due to better utilization of optical power.

2. Methods and Results

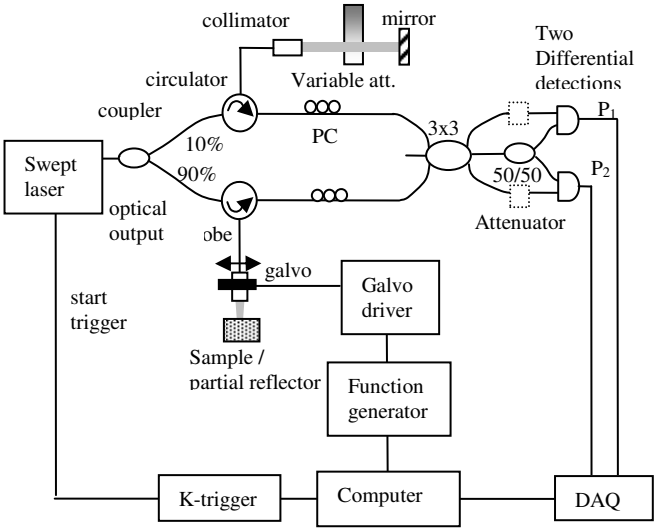

Fig. 1. Schematic diagram of the instantaneous complex conjugate resolved swept-source OCT system using the 3x3 Mach-Zehnder interferometer (MZI) topology with unbalanced (no attenuators) and balanced (with attenuators in the doted line) differential schemes. The coupler ratios of the 3x3 coupler are 0.39/0.29/0.32.

Fig. 1 shows the experimental diagram of the instantaneous complex conjugate resolved swept-source OCT system using the 3x3 Mach-Zehnder interferometer topology with unbalanced and balanced differential detection schemes. A 90/10 2x2 fiber coupler is used as a power divider of the light source: 90% power to the sample and 10% to reference arms. This is an advantage of the MZI, which allows more light to the sample arm for compensating the lower reflection of a biological sample in an OCT system. The 3x3 fiber coupler serves not only as a combiner of the two signals from the sample and reference arms, but also provides three output interferometric signals. To form two channel differential detections, which are needed to obtain the real and imaginary parts of the interferometric signal, one of the output ports of the 3x3 coupler is split using one 2x2 (50/50) fiber coupler. Two differential detections were constructed by combining one output of the 2x2 coupler and one of the remaining outputs of the 3x3 coupler. We note that the input signals for these differential detectors are not balanced, but no optical power is lost. For comparison, an MZI using a commonly used balanced differential detection technique shown in Fig 1 as doted line. In this setup, two additional fiber attenuators were added in the output of the 3x3 coupler. When the detector input power ratio was adjusted to achieve balanced detection, the DC component of the interferometric signal could be dynamically removed, but one third of the optical power would be lost. The swept source (HSL2000, Santac) had a central wavelength of 1320 nm and a full scan wavelength range of 110 nm. The average output power and coherence length of the swept source is 7 mW and 10.8 mm, respectively. A repetition scan rate of 20 kHz was used in our system and the related duty cycle is 68%. Because the swept source operated in the 1300 nm wavelength range, commercial fiber optical coupler, circulator, and polarization controller were available to implement a full fiber based system. The light in the sample arm illuminated a sample through a lensed single mode fiber[15] with a working distance (focus distance to lens surface in air) of 0.9 mm, depth of field (twice the Rayleigh range in air) of 0.4 mm, and $1/e^2$ spot diameter (transverse resolution) of 16 μm. A galvanometer (Blue Hill Optical technologies) scanner scanned the fiber probe light transversely on the sample over 4 mm at 40 Hz with 800 transverse pixels. The total optical power illuminating on the sample was approximately 5 mW. The reference arm was arranged with a fiber collimator and a mirror. A variable attenuator was inserted between the collimator and mirror for adjusting the optical power on reference arm to achieve the shot noise limitation. Two fiber circulators were used in both the sample arm and reference arm to redirect the back-reflected light to a 3x3 fiber coupler. Two polarization controllers (PC) in both reference and sample arms were used for adjustment to match the polarization state of the two arms. Two differential photo-detectors (2117-FC, NewFocus) were used with adjustable band-pass filter and gain. A maximum 3 dB low-pass cutoff frequency of 10 MHz was used in our system. The two detector outputs were digitized using a data acquisition card (DAQ) (PCI 5122, National Instruments) with 14-bit resolution and acquired at a sampling speed of *100 MS/s*. A programmable wave number $k=2\pi/\lambda$ trigger (*k*-trigger) board (HSL-OPK-PKT, Santec) with *17.5 GHz k* interval was used for constant wave number *k* interval trigger. The k-trigger sampling number is 1024. The swept source generated a start trigger signal that

was used to initiate the k-trigger and the function generator for the galvo scanner, in order to initiate the data acquisition process for each A-scan. An average background noise was removed[10,16], before the signal acquisition. A-scans with resolved complex conjugate artifact were obtained by inverse Fourier transformation (IFT). Prior to Fourier transformation, the data set was zero padded to 4096 points resulting in 2048 depth points after Fourier transformation for increasing the resolution[16].

The performance of the complex conjugate ambiguity resolution in our 3x3 Mach-Zehnder SS-OCT systems with the unbalanced configurations could be quantified by comparing the complex conjugate resolved A-scans with the unresolved A-scans. Measurements were taken using a -55dB reflector including coupling loss in the sample arm as shown in Fig. 1. The reference mirror was adjusted to a position such that the difference in optical path length between the two interferometer arms was 300 μm. The extra background noise was subtracted by measuring the reference arm signals with the sample arm blocked. Two output signals P_1 and P_2 from our unbalanced and the commonly used balanced detection SS-OCT system with 3x3 port configuration as $P_{33_1} / P_{33_2} / P_{33_3}$ = 0.39/0.29/0.32 were measured. The peak-peak amplitudes of P_1 and P_2 measured from the unbalanced differential system are 1.9 times higher than that from the balanced differential system. We noticed the DC values of the waveforms in the unbalanced system were removed by the high-pass filter of the detectors. Phase differences between P_1 and P_2 were determined by an optimization method, i.e., by adjusting the phase difference to obtain a minimum of the complex conjugate artifact suppression using the trigonometric relationships[13]:

$$P_{RE}(k) = P_1(k) \tag{1}$$

$$P_{IM}(k) = \frac{P_1(k)\cos(\Delta\phi) - P_2(k)}{\sin(\Delta\phi)} \tag{2}$$

and the inverse Fourier transform of the complex signal $P_{RE}+jP_{IM}$. Phase differences of 90° and 64° were obtained for our unbalanced and the commonly used balanced systems, respectively. The measured results agree very well with the results of our theoretical analysis[17]. A-scans at 300 μm depth was obtained by real inverse Fourier transform of a single detector signal P_1 include the complex conjugate artifact for our unbalanced and the commonly used balanced systems. The symmetric reflective peaks were in both positive and negative sides. The complex conjugate resolved A-scan was obtained by taking the complex inverse Fourier transform directly from our output quadrature signals P_1 and P_2. Suppression of the complex conjugate peaks of 27 dB was obtained at about 300 μm depths in our unbalanced differential detection SS-OCT system. The imaging depth range was double. We found that there is a 7 dB signal-to-noise ratio in our unbalanced differential detection SS-OCT system higher than that in the common used balanced detection method. The suppression of the complex conjugate artifact in our unbalanced detection configurations were 3 dB more than in the commonly used balanced detection method. This is due to better utilization of optical power.

Fig. 2 shows i*n vivo* images of human finger tip acquired by our full range swept-source optical coherence tomography using our 3x3 Mach-Zehnder interferometer with unbalanced differential detection technique. The resolutions of the axial and lateral are 8 and 16 μm, respectively. In Fig. 2 (a), the image was generated using only a single detector, and demonstrates the folded artifact images. In Fig. 2 (b), the complex signal was used demonstrating artifact-free imaging over a depth range of 4 mm.

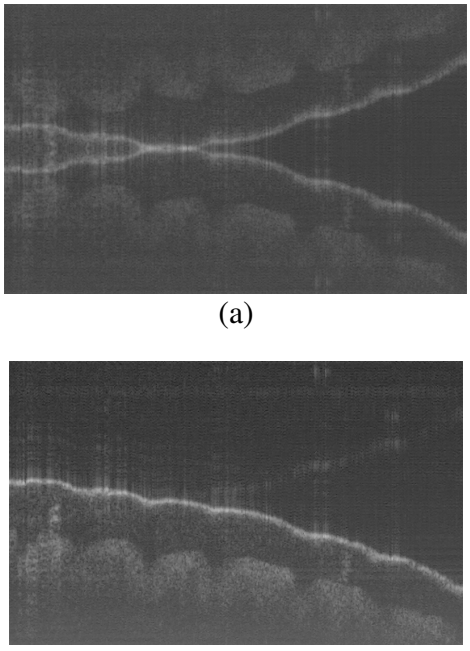

Fig. 2. *In vivo* images of human finger tip acquired by our full range swept-source optical coherence tomography using our 3x3 Mach-Zehnder interferometer with unbalanced differential detection technique. (a): the image was generated using only a single detector. (b): the complex signal was used.

3. Conclusion

We demonstrate a 3x3 Mach-Zehnder interferometer with a new unbalanced differential detection method for full range SS-OCT systems. Using this setup, we achieved a complex conjugate artifact suppression of 27 dB. A 90^{o} phase shift between the two interferometric outputs was obtained thereby eliminating the need for further trigonometric calculations. Also, our setup resulted in a 7 dB increase in the signal-to-noise ratio and 3 dB more in the suppression of the complex conjugate artifact compared to a similar interferometer with the commonly used balanced detection technique.

References

1. D. Huang, E. A. Swanson, C. P. Lin, J. S. Schuman, W. G. Stinson, W. Chang, M. R. Hee, T. Flotte, K. Gregory, C. A. Puliafito, and J. G. Fujimoto, "Optical coherence tomography", Science **254,** 1178-1181 (1991).
2. R. C. Youngquist, S. Carr, and D. E. N. Davies, "Optical coherence-domain reflectometry: A new optical evaluation technique", Opt. Lett., **12**, 158-160 (1987).
3. K. Takada, I. Yokohama, K. Chida, and J. Noda, "New measurement system for fault location in optical waveguide devices based on an interferometric technique", App. Opt. **26**, 1603-1606 (1987).
4. B. E. Bouma and G. J. Tearney, *Handbook of optical coherence tomography* (Marcel Dekker, New York, 2002).
5. R. Leitgeb, C.K. Hitzenberger, and A.F. Fercher, "Performance of Fourier domain vs. time domain optical coherence tomography", Opt. Exp. **11**, 889-894 (2003).
6. M.A. Choma, M.V. Saranic, C. Yang, and J.A. Izatt, "Sensitivity advantage of swept source and Fourier domain optical coherence tomography", Opt. Exp. **11**, 2183-2189 (2003).
7. J.F. de Boer, B. Cense, B.H. Park, M.C. Pierce, G.J. Tearney, and B.E. Bouma, "Improved signal-to-noise ratio in spectral-domain comared with time-domain optical coherence tomography", Opt. Lett. **28**, 2067-2069 (2003).
8. J. Zhang, W. Jung, J.S. Nelson, and Z. Chen, "Full range polarization-sensitive fourier domain optical coherence tomography", Opt. Exp. **12**, 6033-6039 (2004).
9. S.H. Yun, G.J. Tearney, J.F. de Boer, and B.E. Bouma, "Removing the depth-degeneracy in optical frequency domain imaging with frequency shifting", Opt. Exp. **12**, 4822-4828 (2004).
10. B.J.Vakoc, S.H. Yun, G.J. Tearney, and B.E. Bouma, "Elimination of depth degeneracy in optical frequency_domain imaging through polarization-based optical demodulation", Opt. Lett. **31**, 362-364 (2006).
11. M.A. Choma, C. Yang, and J.A. Izatt, "Instantaneous quadrature low-coherence interferometry with 3x3 fiber-optic couplers", Opt. Lett. **28**, 9672162-2164 (2003).
12. M.V. Sarunic, B.E. Applegate, and J.A. Izatt, "Real-time quadrature projection complex conjugate resolved Fourier domain optical coherence tomography", Opt. Lett. **31**, 2426-2428 (2006).
13. M.V. Sarunic, M.A. Choma, C. Yang, and J.A. Izatt, "Instantaneous complex conjugate resolved spectral domain and swept-source OCT using 3x3 fiber couplers", Opt. Exp. **13**, 957-967 (2005).
14. C. Flueraru, H Kumazaki, S. Sherif, S. Chang, and Y. Mao, "Quadrature Mach-Zehnder interferometer with application in optical coherence tomography", J. Opt. A: Pure Appl. Opt. **9**, L5-L8 (2007).
15. Y. Mao, S. Chang, S. Sherif, and C. Flueraru, "Graded-index fiber lens proposed for ultrasmall probes used in biomedical imaging", Apl. Opt. **46**, 5887-5894 (2007).
16. R. Huber, M. Wojtkowski, K. Taira, and J.G. Fujimoto, "Amplified, frequency swept lasers for frequency domain reflectometry and OCT imaging: design and scaling principles", Opt. Exp. **13**, 3513-3528 (2005).
17. Y. Mao, S. Sherif, and C. Flueraru, S. Chang, "3x3 Mach-Zehnder Interferometer with unbalanced Differential Detection for Full Range Swept-Source Optical Coherence Tomography", Apl. Opt. in processing (Manuscript ID: 86374)